

PEROVSKITE/CRYSTALLINE SILICON TANDEMS: IMPACT OF PEROVSKITE BAND GAP AND CRYSTALLINE SILICON CELL ARCHITECTURE

S.L. Luxembourg¹, D. Zhang², M. Najafi², V. Zardetto³, S. Veenstra², L.J. Geerligs¹

¹ECN Solar Energy, P.O. Box 1, NL-1755 ZG Petten, The Netherlands

²ECN-Solliance, High Tech Campus 21, NL 5656AE Eindhoven, The Netherlands

³TNO-Solliance, High Tech Campus 21, NL 5656AE Eindhoven, The Netherlands

ABSTRACT: The combination of a semi-transparent, wide band gap perovskite solar cell (ST PSC) with a crystalline silicon (c-Si) bottom cell in a tandem configuration is considered a promising approach to enhance solar cell efficiencies over the current single junction c-Si cell efficiencies. In this study, we use a simple model based on experimental EQEs and IV-parameters, to predict the 4-terminal tandem efficiency of advanced industrial c-Si cells of different architectures, combined with an experimental 15% ST PSC with a 1.55eV band gap. In addition, we use this model to study the expected effect of the variation of the band gap of the perovskite absorber on the 4-terminal efficiency which results in a positive outlook towards > 25% tandem efficiencies. Furthermore, we demonstrate an experimental 4-terminal tandem efficiency of 24.1% with a MWT-HIT bottom cell.

Keywords: c-Si, Modelling, Perovskite, Tandem

1 INTRODUCTION

With decreasing cell and module prices, balance-of-system (BoS) costs are making up an increasing share of the total costs of photovoltaic systems. Currently, this share is over 50%. Therefore, reduction of BoS-costs is getting increasingly important to lower the cost of solar electricity. Enhancement of solar cell efficiencies is an important driver of BoS-cost reduction. The realization of tandem devices with crystalline silicon bottom cells and wide band gap perovskite top cells is considered a very promising approach towards high efficiency devices. The ongoing increase in the efficiency of perovskite solar cells and the progress being made in terms of their stability draw a lot of attention to this field of research.

Here, we combine an efficient semi-transparent perovskite solar cell (ST PSC) developed within Solliance with several (advanced) industrial crystalline silicon (c-Si) concepts, which have been developed at ECN or in collaboration with external partners. One of these concepts is a silicon heterojunction solar cell, which is generally considered as promising bottom cell technology due to its high overall performance, high V_{oc} and good near-infrared (NIR) response. The specific silicon-heterojunction cell considered here includes metal-wrap-through contacting (MWT-HIT). In a collaborative development with Choshu Industry Co. an efficiency of 23% was realized for this cell concept.[1] In addition, we have included cells with polysilicon (poly-Si) passivating contacts. First, the Passivated Emitter and Rear Polysilicon cell (PERPoly) design with a realized efficiency of 21.5%. PERPoly cells combine a diffused front side emitter with an n++ doped polysilicon (Poly-Si) rear contact, with fire-through (FT) metallization grids.[2] In such a cell structure performance is limited by front surface recombination. In a further development we also consider the implementation of front side poly-Si passivation (two sided poly-Si or 2s-Poly) which reduces front surface recombination. Although, this introduces significant UV-Vis parasitic absorption, this is largely mitigated when implemented as bottom cell in a perovskite/c-Si tandem.[3]

An experimental evaluation of 4-terminal tandem efficiency was performed for a high efficiency MWT-HIT cell. For the other c-Si cell concepts the tandem

efficiency was estimated using a simple modelling approach making use of experimental external quantum efficiencies (EQE). The effect of widening of the perovskite band gap was evaluated on the various cell concepts using the same model.

2 METHODOLOGY

2.1 Semi-transparent perovskite solar cell

A semi-transparent p-i-n perovskite solar cell (ST PSC) including a triple-cation perovskite absorber material with a 1.55 eV band gap was used as top cell in this study. The thickness of the perovskite material was around 570 nm, and the cell size 0.09 cm². This organic-inorganic trihalide perovskite absorber material consists of a mixture of methylammonium (CH₃NH₃, MA), formamidinium (HC(NH₂)₂, FA) and Cs A-site cations which offers enhanced thermal stability and band gap tuning possibilities over the MA tri-iodide absorber [4]. It includes a double (highly transparent) PTAA / NiO_x hole transport layer (HTL) and a double PCBM / ZnO electron transport layer (ETL). More details will be included in a forthcoming publication.

2.2 c-Si bottom cells

Advanced industrial 6 inch n-type c-Si solar cells were prepared in-house or in collaboration with external partners. Details on the 21.9% - MWT-HIT, 21.5% - PERPOLY and 20.0% - 2s-Poly (provided by Tempres, for more information see [5]). SJ IV-measurements and spectral response measurements to determine the external quantum efficiencies (EQE) were performed on these cells. As described below, we have used a simple modelling approach to estimate the 4-terminal tandem efficiencies for the combination of these cells with the ST PSC described above. We derived low-injection level IV-parameters using neutral density filters.

In addition, a 23% MWT-HIT cell which was developed in collaboration with Choshu Industry Co. [1] was used in this study. This cell will be labelled MWT-HIT_I below to distinguish it from the 21.9%-MWT-HIT cell mentioned above, which will be labeled MWT-HIT_{II}. The MWT-HIT_I cell was laminated including front glass and EVA and rear EVA and white reflective back sheet

for the purpose of experimentally determining the 4-terminal tandem efficiency in combination with the ST PSC (see below for details of methodology). As unfortunately, no EQE data of the bare cell was available it was not included in our modelling effort.

2.3 Measurement of tandem efficiency

Due to the large difference in scale of the sub-cells we used an indirect method, previously reported by Werner *et al.*, [6] to determine the 4-terminal tandem efficiency. In short: ST PSC EQE and IV-measurements were performed on a black background. In order to determine the J_{sc} of the c-Si bottom cell the EQE of a laminated cell was measured through a perovskite optical filter. The filter was positioned on top of the c-Si cell using index matching liquid to prevent optical losses. Its V_{oc} and FF corresponding to its operation as bottom cell were obtained by adjusting the solar simulator's light intensity to meet the low injection level operation conditions of the bottom cell. The 4-terminal tandem efficiency is then obtained as the sum of the PSC and filtered c-Si bottom cell efficiencies.

2.4 Modelling of tandem efficiency

4-Terminal tandem efficiencies for several advanced industrial c-Si bottom cell architectures combined with the ST PSC described above were determined from a simple modelling approach based on experimental EQEs. A similar approach was outlined previously in Yu *et al.* [7]. The J_{sc} of c-Si bottom cell was derived from its experimentally determined single-junction (SJ) EQE according to:

$$J_{sc,SJ}(\lambda) = q \cdot EQE_{SJ}(\lambda) \cdot \Phi_{incident}(\lambda)$$

$$f_{bottom}(\lambda) = \frac{\Phi_{bottom}(\lambda)}{\Phi_{incident}(\lambda)}$$

$$J_{sc,bottom}(\lambda) = f_{bottom}(\lambda) \cdot J_{sc,SJ}(\lambda)$$

Here, $J_{sc,SJ}(\lambda)$ corresponds to the short-circuit current density per unit of wavelength of the SJ device under AM1.5 illumination. $\Phi_{incident}(\lambda)$ indicates the AM1.5 photon flux, while $\Phi_{bottom}(\lambda)$ corresponds to the photon flux that reaches the bottom cell. Then $f_{bottom}(\lambda)$ refers to the fraction of $\Phi_{incident}(\lambda)$ reaching the bottom cell and $J_{sc,bottom}(\lambda)$ to the bottom cell short-circuit current density per unit of wavelength. $J_{sc,bottom}$ is obtained from the integration of $J_{sc,bottom}(\lambda)$.

Bottom cell V_{oc} and FF are obtained from low-injection level IV measurements as explained above and combined with the modelled $J_{sc,bottom}$ to arrive at the bottom cell efficiencies. The overall 4-T tandem efficiency was obtained by a lossless addition of the top and bottom cells.

To study the effect of the variation of the perovskite top cell's band gap on the overall tandem and bottom cell efficiency a simple approach was taken. The $f_{bottom}(\lambda)$ as defined above was shifted to mimic the presence of a wider band gap top cell, while the shape of the curve and asymptotic value were preserved. By doing so we implicitly assume that an increase of the perovskite band gap will result in a blue shift of its absorption coefficient and that the parasitic absorption (in TCOs, ETL and HTL) is at a constant level over the considered energy (shift) range. Furthermore, we have assumed a constant transmittance below the band gap by taking a spectrally

weighted average of the transmittance over the below band gap energy range. Examples of $f_{bottom}(\lambda)$ curves resulting from this procedure are included in Fig. 1.

The J_{sc} of the wider band gap PSCs was obtained from a correction of the 1.55eV band gap J_{sc} through calculation of the current density equivalent of the enhanced transmission. V_{oc} and FF values were derived by assuming constant fractions of the Shockley-Queisser [8, 9] limited values. The magnitudes of these fractions were derived from the experimental ST PSC device with 1.55eV band gap.

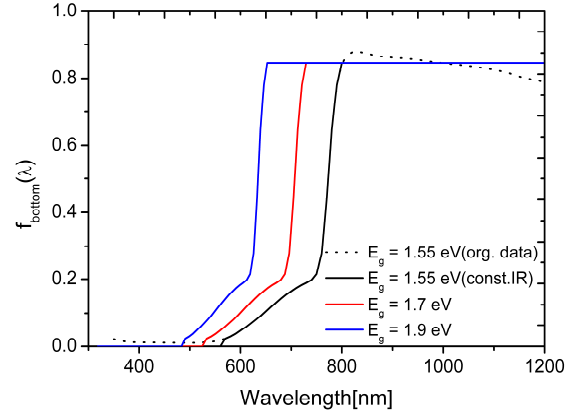


Figure 1: Modelled shift of $f_{bottom}(\lambda)$ with perovskite E_g

3 RESULTS

3.1 Experimental results

The IV-characteristics of the ST PSC are included in Table I. The measurements show low hysteresis, and a stabilized efficiency of 15.0% in a five-minute maximum power point tracking experiment. For preconditioning the cell underwent a 10-minute UV exposure from the glass side. The current ST PSC J_{sc} , V_{oc} and FF values correspond to 0.73, 0.84 and 0.79 of their respective Shockley-Queisser [8, 9] limited values for a band gap of 1.55eV. Below, we use these V_{oc} and FF fractions to estimate PSC and tandem efficiencies for various band gaps. Optical and electrical optimization of the current ST PSC design is expected to result in further efficiency enhancement.

Table I: JV-characteristics of the p-i-n triple-cation ST PSC used as top cell in this study

	J_{sc} [mA/cm ²]	V_{oc} [V]	FF	η [%]
Backward	20	1.056	0.725	15.3
Forward	19.9	1.057	0.716	15
Max. PPT				15

JV-characteristics of the c-Si solar cells which were employed as bottom cell in this study are included in Table II. The variation in V_{oc} among the different devices results from differences in realized recombination currents. As can be expected from the high quality passivation in these devices, the cells with front-and-rear passivating contacts: the MWT-HIT_{II} and the 2s-Poly cells, demonstrate the highest V_{oc} values. The current 2s-Poly cell includes front and rear poly-Si passivating contacts with a thickness of approximately 100 nm. Such thick poly-Si front contact is not optimized for SJ

operation due to the associated large UV-Vis optical losses [3, 10], which are the cause of the relatively low J_{sc} of the 2s-Poly cell. In Fig. 2 EQE curves of the PERPoly, MWT-HIT_{II} and 2s-Poly cells are included. From this figure the low wavelength parasitic absorption in the 2s-Poly cell is apparent, The MWT-HIT_{II} cell shows reduced EQE values in the 800 – 1000 nm range which is expected to result from absorption in the not-optimized TCO layers. The MWT-HIT_{II} and 2s-Poly cells demonstrate the highest EQE in the NIR (above 1000 nm).

Table II: Single-junction JV-characteristics of the c-Si cells used as bottom cell in this study. The cells in the first three rows were used in our modelling approach, while the MWT-HIT_I cell was used in the experimental analysis. The results of the latter were obtained on a single-cell laminate including a 3 mm edge of exposed white back sheet. In the last row the realized JV-characteristics of the MWT-HIT_I as bottom cell are included.

	J_{sc} [mA/cm ²]	V_{oc} [V]	FF	η [%]
2s-Poly	38.2	0.685	0.77	20.0
PERPoly	39.7	0.676	0.80	21.5
MWT-HIT	39.3	0.723	0.77	21.9
MWT-HIT _I	38.9	0.732	0.77	21.8
MWT-HIT _{I,bot}	16.1	0.711	0.80	9.1

The JV-characteristics of the c-Si cells under low-injection level conditions were determined in JV-measurements using a set of neutral density filters to vary the light intensity. These characteristics are used below to calculate the modelled tandem efficiencies below. For the PERPoly and 2s-Poly cells this procedure was performed on laminated cells.

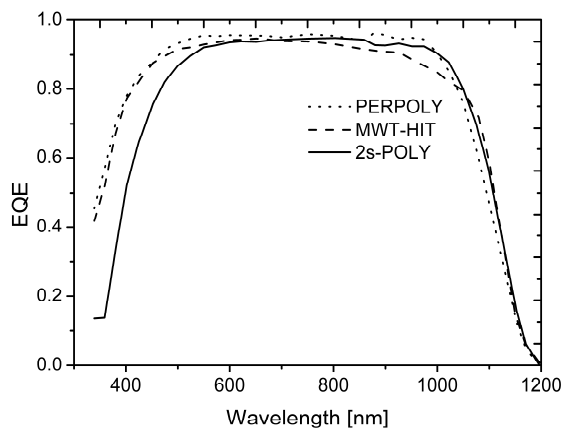


Figure 2: Single-junction EQE curves of the c-Si cells which were evaluated as bottom cell using our modelling approach

An experimental 4-terminal tandem efficiency was determined for the ST PSC joined with the laminated MWT-HIT_I cell obtained as described in the Methodology section. This resulted in a 24.1% tandem efficiency, corresponding to a 2.3%_{abs}-efficiency gain over the SJ MWT-HIT_I efficiency measured on the laminated cell. The MWT-HIT_I SJ and bottom cell (MWT-HIT_{I,bot}) characteristics are included in Table II. The recorded EQE curves are displayed in Fig. 3. From

the comparison of the SJ MWT-HIT_I laminate EQE ($J_{sc} = 38.9 \text{ mA/cm}^2$) to the tandem EQE ($J_{sc} = 35.6 \text{ mA/cm}^2$) it is apparent that there is significant current loss due to parasitic absorption in the charge collecting layers of the top cell. In addition, there is a clear above band gap tail in the top cell transmission, which may be reduced by light management measures such as front surface texturing. $f_{\text{bottom}}(\lambda)$ was determined from these experimental data as the ratio of the bottom cell EQE measured through the perovskite filter (dashed red curve in Fig. 3) to the SJ EQE (solid black curve). The derived $f_{\text{bottom}}(\lambda)$ was assumed to be valid for all c-Si bottom cells considered in this study. In view of the similarities in their cell design this seems a valid assumption.

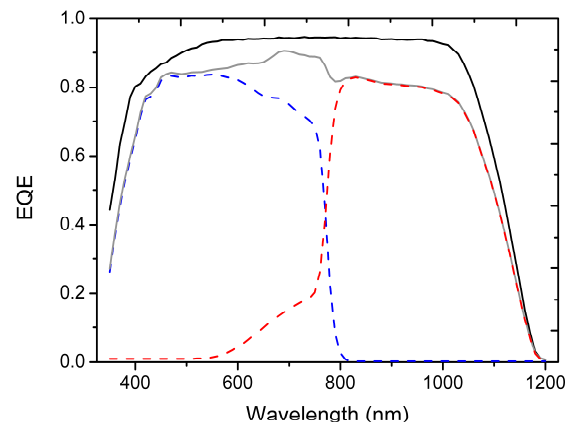


Figure 3: EQE curves of single-junction MWT-HIT_I (solid black) and as bottom cell (dashed red), the ST PSC (dashed blue) and the overall 4-terminal tandem (solid grey)

3.2 Modelled tandem efficiencies

Using the methodology outlined above and the cell parameter inputs as determined in the previous section, we estimated the tandem efficiencies for the c-Si bottom cells included in Table II and the ST PSC described in section 3.1. In addition, we varied the band gap of the perovskite absorber up to 2.0 eV using the methodology described in section 2.4. The resulting tandem efficiencies are included in Fig. 4 as the three lower curves.

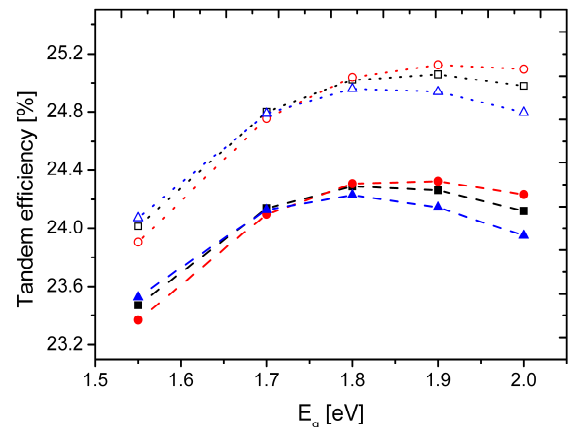


Figure 4: Modelled 4-terminal tandem efficiencies as a function of the ST PSC band gap for a variety of c-Si bottom cells (PERPoly (black), MWT-HIT_{II}(red), 2s-Poly (blue)) for the experimentally determined top cell transparency (dashed) as well as for an increased NIR transparency (dotted).

Although, there is a spread of close to 2% in the SJ efficiencies of the c-Si bottom cells, the differences in tandem efficiencies are only very minor. This is in particular the case for perovskite band gap values in the range of 1.55 – 1.8 eV. At 1.55 eV band gap the predicted tandem efficiencies are all between 23.4 – 23.5%. The 2s-Poly cell, which has the lowest SJ efficiency of the considered cells, is even predicted to have the highest tandem efficiency at this band gap, with a tandem over SJ gain of 3.5%. As was mentioned above the SJ efficiency of the 2s-Poly cell is limited by the UV-Vis parasitic absorption in the front poly-Si layer. In the tandem configuration the perovskite top cell filters and uses this low wavelength range effectively. The 2s-Poly cell shows the best overall NIR response which has the largest impact in combination with the lowest band gap perovskite solar cell. In addition, its FF shows a steeper upward trend than the PERPoly cell with decreasing illumination level (corresponding to decreasing perovskite band gap). This is attributed to a higher realized series resistance of this cell. The 2s-Poly cell was selected for the highest V_{oc} and was somewhat underfired, resulting in a higher contact resistance. The FF of the MWT-HIT_{II} cell studied with the model showed a downward trend of the FF versus illumination level, which is related to a lower shunt resistance.

Under the reduced illumination levels we find for all cells a linear change of V_{oc} with the log of the J_{sc} (see Fig. 5). Since the 2s-Poly cell loses the least in J_{sc} when operated as bottom cell, its reduction in V_{oc} will also be relatively low. The factors mentioned above provide a qualitative insight in the origin of the very similar 4-terminal tandem efficiencies for the different c-Si cells. As for higher perovskite band gap values (and thus higher bottom cell injection levels) the bottom cell JV-characteristics are getting closer to their SJ values. Consequently, the modelled tandem efficiencies are more in line with what would be expected on the basis of the SJ efficiencies (see also Fig. 4).

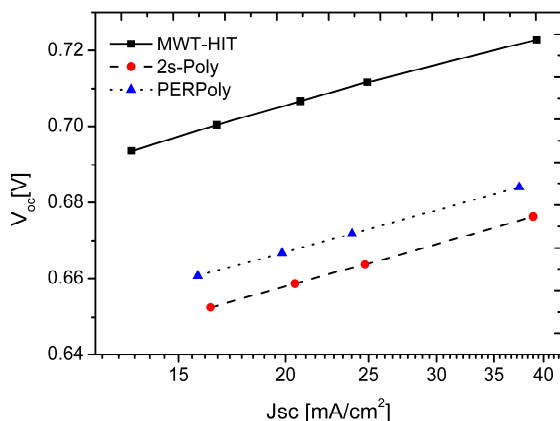


Figure 5: Reduction of V_{oc} with decreasing injection level plotted as function of J_{sc}

Our modelling exercise predicts an approximate 1% gain in tandem efficiency when the PSC band gap is increased to the more optimum values of 1.8-1.9 eV. Here, the model predicts tandem efficiencies of 24.3% for MWT-HIT and PERPoly cell architectures and 24.2% for the 2s-Poly cell, corresponding to tandem over SJ gains of between 2.4% and 4.2%.

The efficiency values in the upper curves have been obtained under the assumption of an increased NIR

transparency of 0.9. Such increased transparency is thought to be realized through reduction of parasitic absorption in particular in the PSC TCOs. A possible route to achieve this could be to replace the current ITO layers by more transparent IO:H layers in future devices.

The modelled increase in transparency should enable tandem efficiencies larger than 25% for the considered c-Si solar cells, which are considered to be advanced but industrial cell architectures. Our on-going work on the improvement of the semi-transparent perovskite to cell will further improve its efficiency, which will facilitate 4-terminal tandem efficiencies beyond the values quoted in this study.

4 CONCLUSIONS

We have demonstrated a 24.1% 4-terminal tandem measurement for the combination of 15% semi-transparent perovskite solar cell and a c-Si MWT-HIT bottom cell. With a simple model based on experimental EQEs we have compared the performance of several advanced industrial c-Si solar cell architectures. Although, single-junction efficiencies of these cells differ by approximately 2%_{abs} the modelled 4-terminal tandem efficiencies for a perovskite band gap of 1.55eV become nearly equal. As discussed in the text this is a consequence of the specifics of the individual cells considered. We show that for an optimal perovskite band gap of 1.8 – 1.9 eV and improvement of the NIR transparency of the top cell from 0.85 to 0.9 tandem efficiencies > 25% are expected. This enhanced transparency corresponds to a reduction parasitic absorption. In addition, the current perovskite cell can be improved in terms of light management and will also benefit from reduction of (TCO) parasitic absorption. From electrical modeling the presence of a significant series resistance in the ST PSC device was identified. In future work we aim to reduce this series resistance by improving the electrode geometry thereby increasing the FF and thus the PCE of the ST-PSC device. These ongoing improvements will enable further increase of the perovskite/c-Si 4-terminal tandem efficiencies.

ACKNOWLEDGEMENTS

We would like to thank Tempres Systems, Vaassen, The Netherlands, and in particular dr. R. Naber, for kindly providing the front-and-rear polysilicon solar cell (2s-Poly) used in this study. In addition, we would like to thank the people at ECN working on the PERPoly cell and MWT-HIT concepts, in particular G. Coletti, M.K. Stodolny and I. Romijn for providing the PERPoly and MWT-HIT cells and Choshu Industry Co. for providing the MWT-HIT_{CIC} cell.

REFERENCES

- [1] G. Coletti, F. Ishimura, Y. Wu, E.E. Bende, G.J.M. Janssen, K. Hashimoto, Y. Watabe, B.B. van Aken, 32nd EU PVSEC (2016).
- [2] M.K. Stodolny, M. Lenes, Y. Wu, G.J.M. Janssen, I. Romijn, J.R.M. Luchies, L.J. Geerligns, Solar Energy Materials and Solar Cells 158 (2016) 24-28.
- [3] S.L. Luxembourg, D. Zhang, Y. Wu, M. Najafi, V. Zardetto, W. Verhees, A.R. Burgers, S. Veenstra, L.J.

- Geerligs, Energy Procedia 124 (2017) 621-627.
- [4] D.P. McMeekin, G. Sadoughi, W. Rehman, G.E. Eperon, M. Saliba, M.T. Hörantner, A. Haghighirad, N. Sakai, L. Korte, B. Rech, M.B. Johnston, L.M. Herz, H.J. Snaith, Science 351 (2016) 151-155.
- [5] R.C.G. Naber, M. Lenes, J.R.M. Luchies, 33rd EU PVSEC (2017) 2DO.3.6.
- [6] J. Werner, G. Dubuis, A. Walter, P. Löper, S.-J. Moon, S. Nicolay, M. Morales-Masis, S. De Wolf, B. Niesen, C. Ballif, C. Solar Energy Materials and Solar Cells 141 (2015) 407-413.
- [7] Z. Yu, M. Leilaoui, Z. Holman, Nature Energy 1 (2016) 1-4.
- [8] W. Shockley, H.J. Queisser, Journal of Applied Physics 32 (1961) 510-519.
- [9] S. Rühle, Solar Energy 130 (2016) 139-147.
- [10] S. Reiter, N. Koper, R. Reineke-Koch, Y. Larionova, M. Turcu, J. Krügener, D. Tetzlaff, T. Wietler, U. Höhne, J.-D. Kähler, R. Brendel, R. Peibst, Energy Procedia 92 (2016) 199-204.